THE 4TH INTERNATIONAL CONFERENCE ON ALUMINUM ALLOYS

COMPARISON OF COMPRESSION AND TORSION RESULTS WITH SINH AND POWER LAW CONSTITUTIVE ANALYSES FOR AN 8090 Cr/Mn ALLOY

H.J. McQueen[1], V. Jain[2], A. Hopkins[2], E.V. Konopleva[1] and P. Sakaris[1]

1. Mech. Engr., Concordia University, Montreal, Canada, H3G 1M8
2. University of Dayton Research Institute, Dayton, Ohio, 45469-0130, U.S.A.

Abstract

The alloy Al-2.01Li-1.1Cu-0.89Mg-0.14Cr-0.52Mn was deformed in torsion to fracture and in compression to $\varepsilon = 1.4$ in the ranges of 300 - 550°C and 10^{-2} - 10 s^{-1}. The compression results were analyzed by means of a power -Arrhenius relationship. The compression and the torsion results were subjected to a $(\sinh \alpha \sigma)^n$ -Arrhenius analysis, with variation of the stress multiplier α from 0.01 to 0.08 MPa^{-1} which caused the stress exponent n to decrease at a declining rate and Arrhenius slope s to rise linearly, thus causing the activation energy Q_{HW} to rise towards a stable value. The two test techniques gave very similar flow stresses and constitutive constants. The activation energies from the two modes of analysis show only minor differences. Examination of quenched and anodized specimens exhibited elongated grains with substructure and confirmed that the softening was dynamic recovery.

Introduction And Objectives

Aluminum alloys containing Li with other elements have been subjected to intense research in the past decade because of the promise of markedly increased modulus and decreased density at constant strength [1-3]. The goal has been elusive because of difficulties of ensuring the degree of isotropy, toughness and fatigue resistance comparable to alloys currently employed. Research has been undertaken into the hot workability of several alloys of the 8090 type with variations in the dispersoid inducing elements Zr, Mn and Cr. Such additions are expected to cause minor variations in the hot strength but much stronger effects on ductility and on the ease of recrystallization (SRX) after straining, which is important in avoiding a pancaked grain structure which gives poor through-thickness properties.

The torsion and compression testing, presented with special emphasis on the former, were conducted on the 8090-CrMn alloy, which was provided by Kaiser Aluminum Co. and had the composition listed in Table 1, along with other alloys to be discussed. The as-cast alloys were homogenized at 538°C for 16 hrs. and then air cooled. The torsion tests were carried out on a computer-directed, servo-controlled, hydraulically-powered torsion machine [4,5]. The tests were conducted to fracture or to a true strain of 4 on the matrix 0.1, 1 and 5 s^{-1} and 300, 400 and 500°C. The specimens were rapidly heated in a radiant furnace in an argon atmosphere to deformation temperature, T and held for 5 minutes before testing. The data were converted to equivalent strain ε and stress σ by the following formulae [4,5]:

$$\dot{\varepsilon} = (r / \sqrt{3}L)(\text{angular velocity, radians / s}) \qquad (1)$$

$$\sigma = (\sqrt{3} / 2\pi r^3)(\text{torque})(3 + n'' + m') \qquad (2)$$

where r is gage radius (3.17mm) and L is gage length (17.5mm). The stress corresponding to the surface strain rate is calculated from torque, with the corrections for the gradient in strain and strain rate, which are given by the strain hardening rate n'' (set at zero for σ_m) and by the strain rate sensitivity m'' (d log (torque)/d log $\dot{\varepsilon}$). The compression tests on an MTS hydraulic machine were carried out in air, at constant strain rate on specimens 19.1 mm by 12.7 mm diameter. The test matrix included the ranges 0.01, 0.05, 0.1, 0.5, 1.0, 5 and 10s^{-1} and 300, 350, 400, 450, 500 and 535°C to a strain of about 1.4. The specimens were heated at a rate of 10°C/min. in a split-resistance furnace and held at temperature for 15 min.

The constitutive analysis was based on the following formula [4-11]:

$$A(\sinh \alpha \sigma_m)^n = \dot{\varepsilon} \exp(Q_{HW} / RT) = Z \qquad (3)$$

where, σ_m is the steady state or maximum stress, R, the gas constant and Z, the Zener-Hollomon parameter (combining the control variables T, $\dot{\varepsilon}$), A, α, material constants, n, the stress exponent and Q_{HW}, the apparent activation energy. The value of α is varied from 0.01 to 0.08 MPa^{-1} including 0.052 MPa^{-1}, which is commonly used for Al alloys [7-10]. The data were also analyzed by the power law [12-13].

$$A' \sigma_m^{n'} = \dot{\varepsilon} \exp(Q'_{HW} / RT) \qquad (4)$$

and the material constants from both analyses are compared. The specimens (after polishing and anodizing) were examined by polarized optical microscopy (POM), to determine whether restoration had taken place by dynamic recovery (DRV), marked by elongated grains with substructure, or by dynamic recrystallization (DRX), having equiaxed grains with substructure [8,9,14]. After deformation, the torsion specimens had been withdrawn longitudinally and cooled in a water spray within 3 s. They were cut parallel to the axis to expose a tangential view of the gage length and adjacent section of the shoulder. The compression specimens, removed by opening the furnace, were dropped quickly into the cold water.
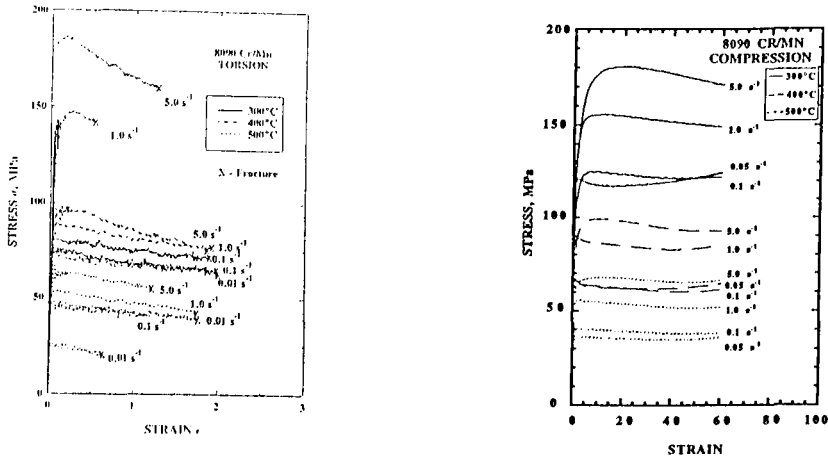
Figure 1: Representative elevated T flow curves for as-cast and homogenized 8090-CrMn: a) torsion tests and b) compression tests.

Results

A selection of flow curves for 8090-CrMn are presented in Figure 1. The torsion test, extending to about $\varepsilon = 2$, exhibit slight peaks and a gradual decline towards steady state regime. The ductility was highest at 400°C, increasing with diminishing $\dot{\varepsilon}$. At 500°C, the ductility was somewhat reduced going through a maximum at 1.0 s⁻¹. The compression tests, extending to $\varepsilon = 1.4$, monatonically attain a steady state. The maximum stress σ_m in each flow curve for both torsion and compression was plotted according to Equation 1, illustrated in Figures 2 and 3. As the value of α was altered through the range 0.01, 0.02, 0.04, 0.052 and 0.08 MPa⁻¹, the slopes in Figure 2 declined and the constant T lines displaced to higher values of $\sinh\alpha\,\sigma$. The slopes in Figure 3 increased and the constant $\dot{\varepsilon}$ lines displaced to higher values of $\sinh\alpha\,\sigma$. For each value of α, the slopes in Figure 2 of the best-fit, constant-T lines were determined and n_{av} evaluated, similarly the slopes in Figure 3 of the best-fit, constant-$\dot{\varepsilon}$ lines were used to evaluate s_{av}. The variation of n and s with α are portrayed in Figures 4 and 5: 1) n, which increases with rising T, decreases at a declining rate, with minimum variation at 0.01 MPa⁻¹ for torsion and
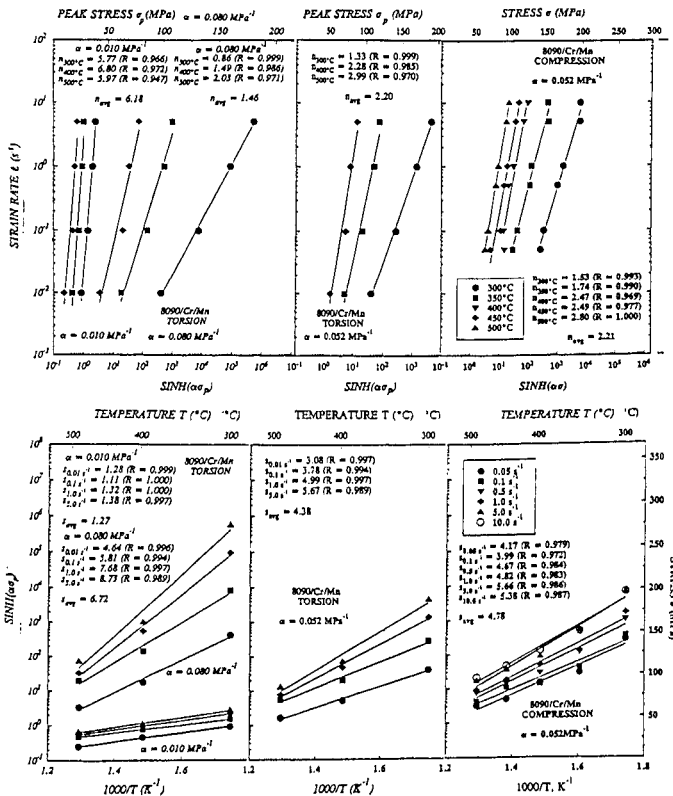
Figure 2: Dependence of σ and $\dot{\varepsilon}$ according to Equation 1 for 8090-CrMn torsion: a) $\alpha = 0.01$ and 0.08 MPa⁻¹, b) $\alpha = 0.052$ MPa⁻¹ and c) compression, $\alpha = 0.052$ MPa⁻¹.

Figure 3: Dependence of σ and T according to Equation 1 for 8090-CrMn torsion: a) $\alpha = 0.01$ and 0.08 MPa⁻¹, b) $\alpha = 0.052$ MPa⁻¹ and c) compression, $\alpha = 0.052$ MPa⁻¹.
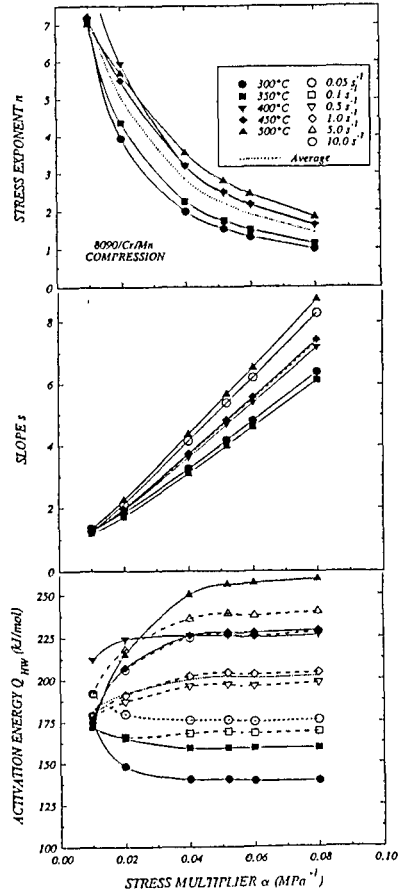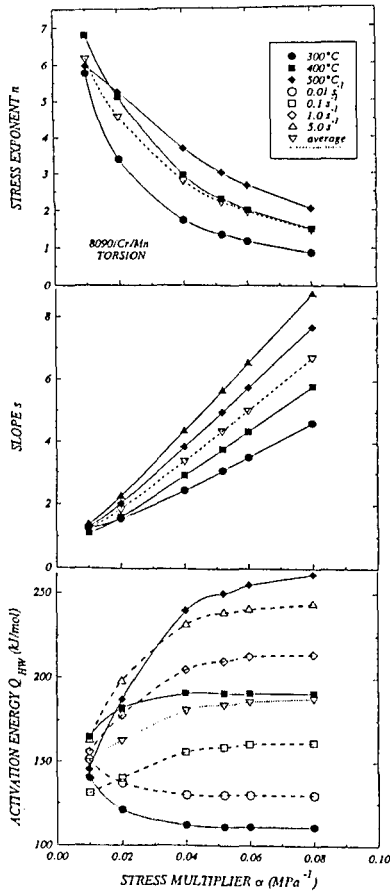
Figure 4: For torsion tests analyzed by Equation 1, the variation with α of a) stress exponent n b) Arrhenius slope s and c) activation energy Q_{HW}.

Figure 5: For compression tests analyzed by Equation 1, the variation with α of a) stress exponent n b) Arrhenius slope s and c) activation energy Q_{HW}.

Table 1: Constitutive Constants And Compositions For 8090 Al-Li Alloys

α	8090Cr/Mn†						8090Zr‡		8090A†‡		Mn	Zr	A
	Torsion			Compression			Tor.	Comp.	Tor.		†	‡	†‡
	Q_{av}	A	r_z	Q_{av}	A	r_z	Q_{av}*	Q_{av}	Q_{av}#				
MPa¹	kJ/mol			kJ/mol			kJ/mol		kJ/mol			wt%	
0.01	150	4.6 x 11	0.990	182	1.4 x 14	0.993	234	188	202	Li	2.01	2.06	2.5
0.02	163			192			194	197	183	Cu	1.10	1.15	1.4
0.04	181	4.7 x 10	0.975	200	1.0 x 12	0.980	178	205	181	Mg	0.88	0.87	0.6
0.052	184	1.7 x 17	0.972	202	8.7 x 11	0.980	176	205	182#	Cr	0.14	-	-
0.06	186			201			176	207	183	Zr	0.02	0.08	0.08
0.08	188	4.7 x 10	0.972	202	5.2 x 11	0.978	176	207	184	Mn	0.52	-	-

* # For 400, 500°C only, when including 300°C, then Q_{HW} = * 317 kJ/mol or # 329 kJ/mol.

at 0.08 MPa^{-1} for compression and 2) s, which generally mounts with rising $\dot{\varepsilon}$, increases almost linearly, with minimum variation for both modes at 0.01 MPa^{-1}. The values of Q_{HW} (2.3 R n s) were calculated for each value of α for all combinations of n with s_{av} and s with n_{av} [7] (Figures 4c and 5c); in both cases, Q_{HW} increases with α to become stable (0.04-0.08 MPa^{-1}): from 150 to 184 kJ/mol for torsion and from 182 to 202 kJ/mol for compression. The values of Q_{HW} for each α were then employed to create plots of log Z vs. log(sinh$\alpha\sigma_m$), as portrayed in Figure 6, which shows that lines displace to higher Z and higher (sinh$\alpha\sigma$) as α increases. The values are established for A, (the intercept) and the correlation coefficients r (Table 2), which are highest for α = 0.01 MPa^{-1}, where it can be seen that the data form a straight line, without curvatures at the extreme points, as is clearly noticeable at higher α.

The compression data were also analyzed by the power law (Figure 7) [12-13]. In the log σ-log $\dot{\varepsilon}$ plots, the constant T data were linear, but the values of n' increased from 6.21 to 11.7 as T declines, which average 2.21 at high σ (300-400°C) and 2.99 at low σ (450-535°C). In the Arrhenius plot, the constant ε data have slopes s', which average 2.21 at high σ and 2.99 at low σ (0.01 - 0.03 s^{-1}). The value of Q' (2.3 R n s) is evaluated to be 186 kJ/mol at high stress and 182 kJ/mol at low stress. The value of Q_{HW}' was also evaluated as $d\ln\dot{\varepsilon}/d(1/T)$, at several constant stresses to be 195 kJ/mol. For the compression specimens, an investigation by POM confirmed the presence of elongated grains. For torsion, the POM micrographs, over the complete range of T and $\dot{\varepsilon}$, exhibited elongated grains as illustrated in Figure 8; the equiaxed shoulder grains are seen to turn into the helicoidal gage grains. At high magnification, it was still not possible to distinguish the subgrains; however, examination by TEM clarified the presence of subgrains [15].

Discussion

The decrease in strain hardening rate and in the steady state flow stress as T rises and $\dot{\varepsilon}$ falls, are strong indication of DRV as the sole restoration mechanism.
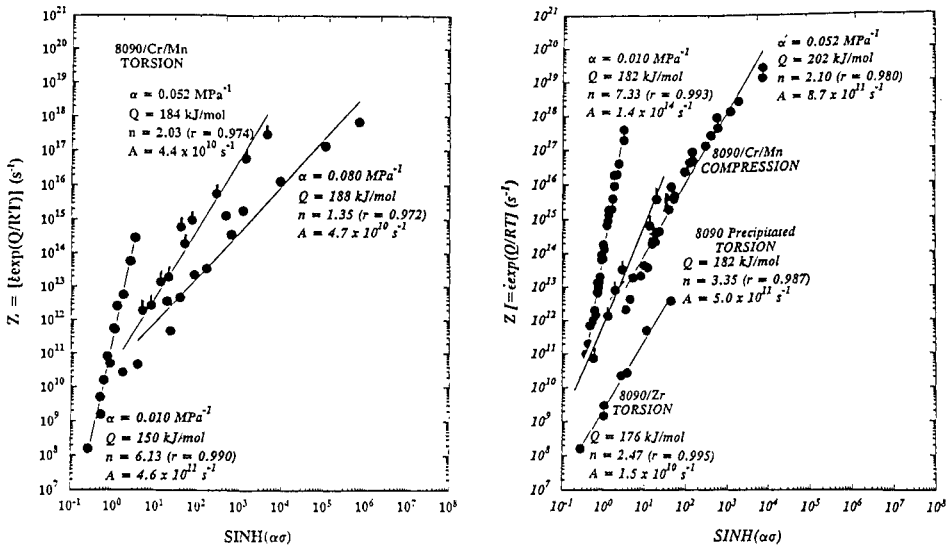
Figure 6: The dependence of stress on the Zener-Hollomon parameter: a) torsion for α = 0.01, 0.052 and 0.08 MPa^{-1} and b) compression for α = 0.01 and 0.052 MPa^{-1}, with comparison to 8090-Zr and to 8090A [5] torsion.

The declines in the flow curves at higher $\dot{\varepsilon}$ and lower T are partially related to deformation heating and partially to coarsening of fine precipitates, which have dissolved at higher T. The degree of softening is likely to be less in compression because of the longer heating time, which improves structural stabilization at the deformation temperature. Peaks followed by work softening have been observed in previous testing of Al-Li alloys [5,6,16-18], notably when the prior heat treatment produced a high solute level so that there was dynamic precipitation [5,6,11,16]. The 8090A had high peaks in the solutioned condition, but in a precipitated condition reported here (Figures 2, 3), had moderate peaks more similar to the present alloy. The ductility in the as-cast condition is relatively low compared to the 8090A taken from rolled plate, where fracture strains were over 2 at 300°C and over 4 at 400 and 500°C [5,6]. The micrographs (Figure 8) confirm the absence of DRX and the TEM, reported separately [15], exposes subgrains which are larger and more perfect, as T rises and $\dot{\varepsilon}$ falls. The operation of DRV as the sole restoration mechanism has been clearly proven in the hot working of 8090A [6] and other Al-Li alloys [16-19].

The suitability of the sinh-Arrhenius Equation 1 was to be expected, since it has been used for many other Al alloys [5,7-11]. To facilitate comparison, $\alpha = 0.052$ MPa^{-1} was initially employed. The values of 184 and 202 kJ/mol are considerably higher than commercial Al (150 kJ/mol), but are in line with many commercial alloys [7-11]. The difference between the two test modes arises from fairly minor differences in the measured stresses: in Table 2, it can be seen that the n ($\alpha = 0.052$ MPa^{-1}) values are almost identical and the s values differ by 10% because the low T compressions are slightly higher and the high T, slightly lower. Upon initial comparison with 8090A, there appeared to be a large discrepancy (329 kJ/mol), which was evidently due to the moderate peaks at 300°C [5,6]. The flow stresses at 400 and 500°C were quite similar and the Q_{HW} for that range (182 kJ/mol) was quite similar. In the present testing program, the values agree quite well with 8090-Zr in Table 1; the 176 kJ/mol for torsion is a little low but it is only for the 400-500°C, since some precipitation and a high peak occurred at 300°C giving 317 kJ/mol (similar to the 8090A) [5,6]. The C155 (2.1Li-2.7Cu-0.3Mg-0.7Zn-0.4Mn-0.04Zr), also tested in the
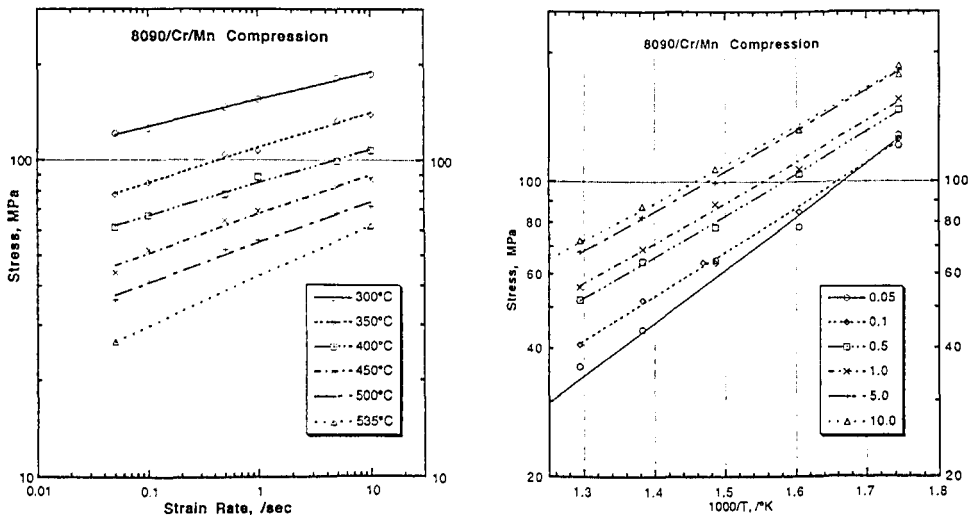
Figure 7: Dependence in hot compression of σ according to the power law (Equation 2): a) on $\dot{\varepsilon}$, the stress exponent n' decreases as T rises and b) on T.

present program, had much higher values (219 and 238 kJ/mol for torsion and compression) than the 8090-CrMn. For Al-2.2Li-1.3Cu-1.2Mg-0.14Zr, Nikura et al. [16] in a power law analysis found Q = 183 kJ/mol. Parsons and Sheppard [17] determined 153 kJ/mol (α = 0.025 MPa^{-1}) for Al-2.4Li-0.9Cu-3.5Mg-0.15Zr and 168 kJ/mol (α = 0.33 MPa^{-1}) for Al-2.2Li-3.6Mg-0.15Zr), somewhat lower than the present results. The high activation energies, compared to that of Al indicate that DRV is impeded by complex interactions between dislocations, particles and solute [11,21]. Industrially, a higher Q_{HW} indicates that in a conventional rolling schedule with declining T, the finishing passes will require higher forces.

The effects of α variation on n and s (Figures 4, 5) are to be expected from the nature of the sinh($\alpha\sigma$) function. The decrease at declining rate for n and the linear increase for s agree with results for other alloys [7]. The initial rapid change and final saturation for Q_{HW} is in agreement with previous analysis, which led to the recommendation that α should be in the range 0.04 to 0.08 MPa^{-1} in order to facilitate comparison between different alloys [7]. However in that study, the initial variation in Q_{HW} was sometimes an increase as here and sometimes a decrease [7]. In fact for the alloys being considered in Table 1, the 8090-A and the torsion results for 8090-Zr exhibit Q_{HW} initially falling; there seems to be no physical explanation for this just the relative changes in the values of n and s. The significance of changing α is seen in Figure 6, where the Z plot is a perfect straight line for 0.01 MPa^{-1} with a high correlation factor; this value is obviously the best choice for modeling purposes. However, it clearly is not the best for comparing Q_{HW}, either for the present alloys as can be realized by consulting Table 2, or in general [7].

In the power law analysis, the value of n' is seen to rise considerably as the temperature is decreased from 535 to 300°C. These values from 6.2 to 11.7 are considerably higher than the common value of about 5 observed in creep at much lower stresses. The variation of n is not extraordinary from a theoretical view point but it obviously makes modeling more difficult. The values of s also vary with $\dot{\varepsilon}$ which is not usual in creep. Despite these problems, it was possible to obtain Q_{HW} values of about 186 kJ/mol consistent with the sinh analyses. It should be noted that the n values are quite different in the two analyses because of the intervening sinh$\alpha\sigma$ function. It is interesting to note that the ideal value of n (~5) is attained at α = 0.02 MPa^{-1} where the Q_{HW} values are in the rapid variation mode. At α = 0.01 MPa^{-1}, the values of n and n' (Table 2) are about the same and the values of Q_{HW} and Q_{HW}' are almost the same; this is a novel observation.
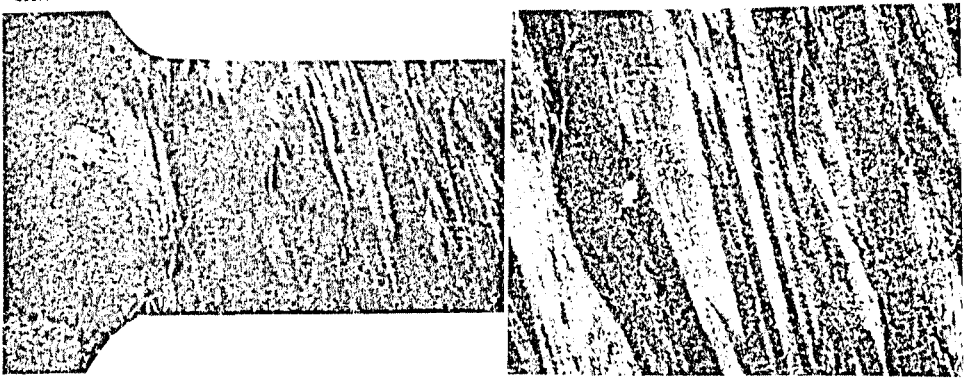
Figure 8: Microstructures by POM after torsion to $\varepsilon \approx 2$ at 400°C: a) 0.01 s^{-1}, shoulder (equiaxed grains) and gage tangential section (X16) and b) 0.1 s^{-1} helicoidal grains observed tangentially in the gage length (X400).

Conclusion

The high temperature flow stresses for 8090-CrMn alloy measured in torsion and compression were very similar; the differences could be ascribed to the different pre-heating rates employed. Because of the heat treatment employed, the initial peak and work softening were smaller than observed in some previous hot workability of Al-Li alloys. Dynamic recovery was the sole restoration mechanism operating during straining. The sinh-Arrhenius constitutive analysis resulted in fairly similar values of n, s and Q_{HW} at $\alpha = 0.052 MPa^{-1}$; the Q_{HW} showed reasonable consistency with other Al alloys. The best-fit of the constitutive analysis was found at $\alpha = 0.01 MPa^{-1}$, because of the high stresses at low T relative to pure Al. However at such low α, the values of Q_{HW} diverged further for the two test modes and even more for comparison with a similar alloy, 8090-Zr. The power law analysis has the difficulty that the stress exponent varies from 6.2 to 11.7. However, the activation energy is reasonably similar to that from the sinh analysis, notably at $\alpha = 0.01 MPa^{-1}$, where stress exponents also agree.

References

1   W.S.Miller, J.White and D.J.Lloyd, Aluminum Alloys: Physical and Mechanical Properties,E.A.Starke and T.H.Sanders,eds.,EMAS Worley,UK,1986,pp.1799-1836.
2   M.A. Reynolds, A. Gray, E. Creed, R.M. Jordan and A.P. Titchener, Aluminum-Lithium Alloys III, C.Baker et al., eds. Inst. of Metals, London, 1986, pp.199-212.
3   J. Wadsworth, C.A. Henshall and T.G. Nieh, Reference [2], pp. 199-212.
4   K. Conrod and H.J. McQueen, Reference [1], pp. 435-447.
5   I.C. Smith, G. Avramovic-Cingara and H.J. McQueen, Aluminum-Lithium Alloys, T.H.Sanders, E.A.Starke,eds., MCPE Pub.,Birmingham,UK, 1989, pp.223-232.
6   G. Avramovic-Cingara, H.J. McQueen and G.L. L'Esperance, Proc. European Conf. Advanced Materials and Processes, 1990, pp. 1305-1310.
7   H.J. McQueen and P. Sakaris, Aluminum Alloys: Physical and Mechanical Properties, (ICAA 3), L. Arnberg et al., eds., NIH-Sinteff, Trondheim, Norway, 1992, Vol. 2, pp. 179-184.
8   H.J. McQueen and K. Conrod, Microstructure Control in Aluminum Alloys, E.H.Chia and H.J.McQueen, eds., TMS-AIME, Warrendale, PA., 1986, pp.197-219.
9   H.J. McQueen, Hot Deformation of Aluminum Alloys, T.G. Langdon et al., eds., TMS-AIME, Warrendale, PA., 1991, pp. 31-54.
10 H.J. McQueen and N. Ryum, Scand. J. Met., 14 (1985), pp. 183-194.
11 H.J. McQueen, Reference [9], pp. 105-120.
12 W. Blum, Reference [9], pp. 181-210.
13 H.J. McQueen, W. Blum, Q. Zhu and V.Demuth, Advances in Hot Deformation, Textures and Microstructures, T.R. Bieler et al. eds., TMS-AIME, Warrendale, PA., 1994, (in press).
14 H.J. McQueen, E. Evangelista, N. Jin and M.E. Kassner, Reference [13], (in press).
15 G. Avramovic-Cingara, A. Hopkins, H.J. McQueen and D. Perovic, (ICAA4).
16 M. Nikura, K. Takahashi and C. Ouchi, Reference (2), pp. 213-221.
17 N.C. Parson and T. Sheppard, Reference [2], pp. 222-232.
18 T. Sheppard, M.J. Tan, H.M. Flower and A.K. Mukhopadhyay, Proc. 4th Int'l. Al Extrusion Seminar, Aluminum Assoc., USA, 1988, Vol. 2, pp. 161-170.
19 S.J. Hales and P.N. Kalu, Reference [13], (in press).
20 E. Evangelista, E. DiRusso, H.J. McQueen and P. Mengucci, Homogenization and Annealing of Al and Cu Alloys, TMS-AIME, Warrendale, PA., 1988, pp. 209-226.
21 B. Verlinden, P. Wouters and H.J. McQueen, Mat. Sci. Eng., A123, (1990), pp. 229-237 and 239-245.